

CHAPTER V

CO-EXTRUSION OF OPTICAL FIBERS

5.1 Abstract

Optical fibers were produced by co-extrusion technique. The polycarbonate (PC) was used as a core material. The 10%, 20% and 25% PASE/PMMA blend were used as cladding materials. The SEM image and DSC thermogram demonstrated that the blendings have no phase separation and they are miscible blend. Co-extrusion process require that the same temperature core material be coated with cladding material inside co-extrusion die and then both of them concurrently extruded through the co-extrusion die. The die zone temperatures is 225 ° C. The piston speeds of melt-spinning and draw ratios were varied. The diameter of fibers decrease when draw ratio increase and the cladding thickness increase when piston speed increase. The PASE/PMMA clad-fibers are more ductile than pure PMMA clad-fibers. However, they exhibit brittleness and also make the PC core fiber become brittle.

5.2 Introduction

Now various series of POF products including GI type POF, SI type POF, fluorescent POF, non-linear POF, etc. have been developed, which are widely used in the fields of light and image transmitting, sensing, and information transmission in short distance. The most typical method of POF is so called continuous co-extrusion process developed by Mitshubishi Rayon Co. A continuous co-extrusion and coating process for making POF has been developed in the earlier 90's of last century by Nanjing Fiberglass Research & Desigh Institute. In 2001, Sohn I.S. and coworkers introduced a coextrusion method using a specially designed coextrusion die which includes two rotating element. In their method, two polymer with different refractive indices are introduced to the special die.

The co-extrusion process produces the core and simultaneously coats it with cladding material. Since two materials are different in melt index, processing

temperature and pressure, viscosity and shear stress, the important of material study should be optimized such as: temperature, screw speed, drawing speed.

This chapter aims to prepare and characterize PASE/PMMA cladding and to fabricate the fiber by co-extrusion process and study the effect of piston speed and draw ratio on the morphology and mechanical properties of the fibers.

5.3 Experiment

The polycarbonate core (PC, wonderlite® PC 110) was dried at 120 °C 5 hours, PASE/PMMA blend and PMMA were dried at 80 °C for 12 hours and immediately used.

The cladding was prepared by blending PASE with PMMA at 10%, 20% and 25% by weight of PASE in Barbender Mixer N50 with Oil bath circulation T300 B at 175 °C, 60 rpm of rotor speed for 20 minutes. The viscosity of PC, PMMA and PASE/PMMA blend were determined by capillary rheometer. The processing temperature of single screw from feed zone to die zone is 275, 285, 280 and 225 °C. The barrel temperature of melt-spinning is 235 °C. The tightly packed-claddings were held in the barrel at that temperature for 3 minutes before spinning. The PC and cladding were then co-extruded in different piston speed (20 and 24.5 mm./min), different draw ratio (free falling and 20 rpm) and constant screw speed (3 rpm). The co-extruder consists of single screw extruder and melt-spinning using a same die. The diameter of single screw die which is used to form core part is 1 mm. The circular sheath die has 0.7 mm width. The single screw has 19 mm. diameter, 500 mm. length and 2:1 compression ratio. A barrel diameter of melt-spinning is 2.2 cm and the length is 15 cm. The rotor has cross section equal to 56.768 cm².

Thermal properties of the blending were determined by DSC and TGA. Morphologies were studied by JSM-6400 Model Scanning Electron Microscope (SEM). The diameters of core and the thickness of cladding were determined by Leica DMXDP optical microscope (OM) at the magnification of 4x and 20x. The tensile strength and the elongation at break of fibers were estimated by LLOYD universal tensile testing machine with 5 mm/min crosshead speed, 2.5 kN load cell with 5 cm gauge length

5.4 Results and Discussion

5.4.1 PASE/PMMA blend

The PASE was blended with PMMA in the ratio of 10%, 20% and 25% by weight. Figure 5.1 shows the picture of the blending. SEM images show that they do not have phase separation as show in figure 5.2. The glass transition temperature (T_g) of PASE/PMMA blend at every ratios is lower than T_g of PMMA because of the flexible of siloxane linkage (see in figure 5.3). T_g of 10%, 20% and 25% PASE/PMMA is 92.37, 90.26 and 93.0 °C, respectively (Fig. 5.3). T_g of 25% PASE/PMMA is not sharp. The changing in T_g of pure PMMA component indicating that the blendings are miscible. The decomposition temperatures (T_d) from TGA of the blendings are higher than PMMA but less than PASE (see in figure 5.4). 10% and 20% of PASE/PMMA blend decomposed at 362.8 °C and 369.4 °C respectively. 25% PASE/PMMA gradually decomposed at about 280 °C which is resulting from the higher content of PASE and then rapidly decomposed of PMMA component at about 360 °C. The residue weight of three blendings is about 10% at 700 °C which belong to silicon and some aromatic content. Figure 5.5 show DSC and TGA thermograms of PC core. T_g and T_d of all materials were shown in the table 5.1.

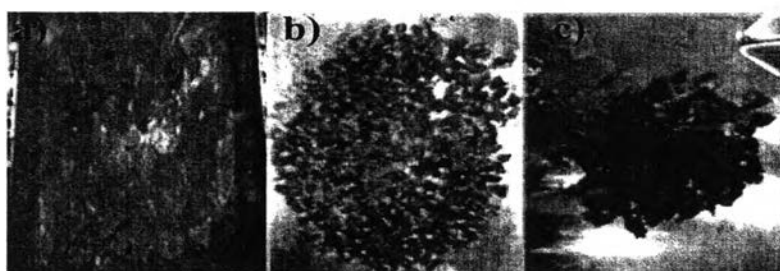


Figure 5.1 Picture of PASE/PMMA blend a) 10 % PASE/PMMA, b) 20 % PASE/PMMA and c) 25% PASE/PMMA.

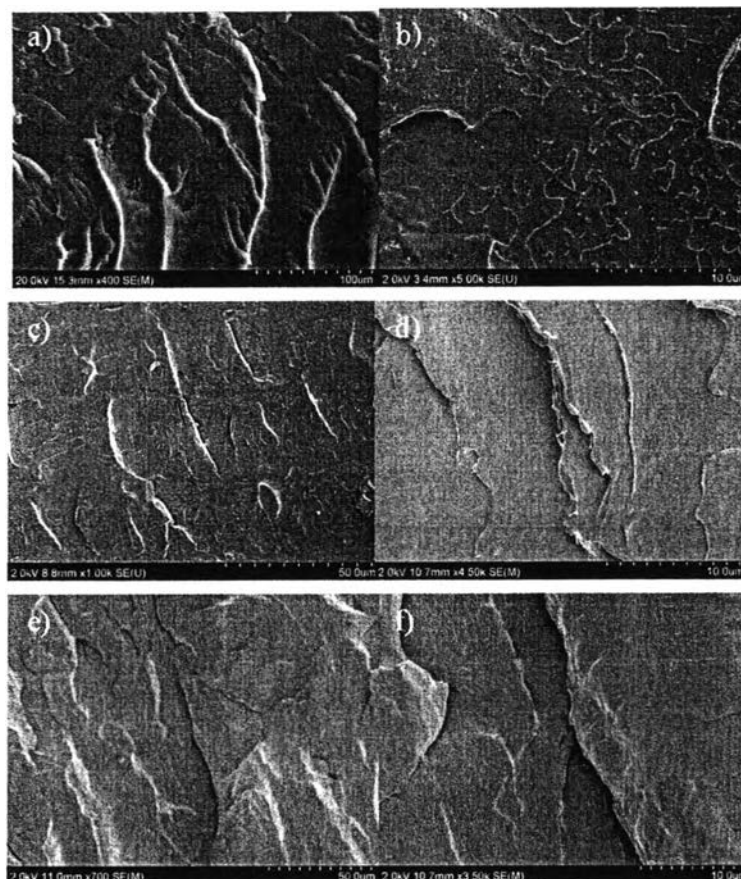


Figure 5.2 SEM images of 10 % PASE/PMMA (a) 100 μm ., b) 10 μm .), 20 % PASE/PMMA (c) 50 μm ., d) 10 μm .) and 25% PASE/PMMA (e) 50 μm ., f) 10 μm .).

Table 5.1 Summary of the thermal properties of PMMA, PC and PASE

Materials	T_g ($^{\circ}\text{C}$)	T_d ($^{\circ}\text{C}$)
PC	149.33	495.8
PMMA	103.5	353.2
PASE	47.61	391.0
10% PASE/PMMA	92.37	362.8
20% PASE/PMMA	90.26	369.4
25% PASE/PMMA	93.0	280, 360

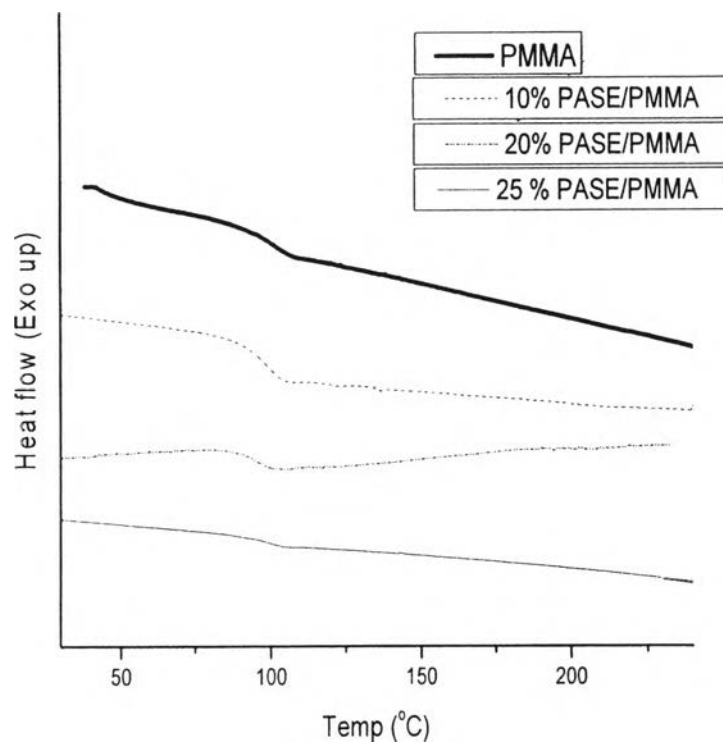


Figure 5.3DSC thermogram of claddings— PMMA and PASE/PMMA blends.

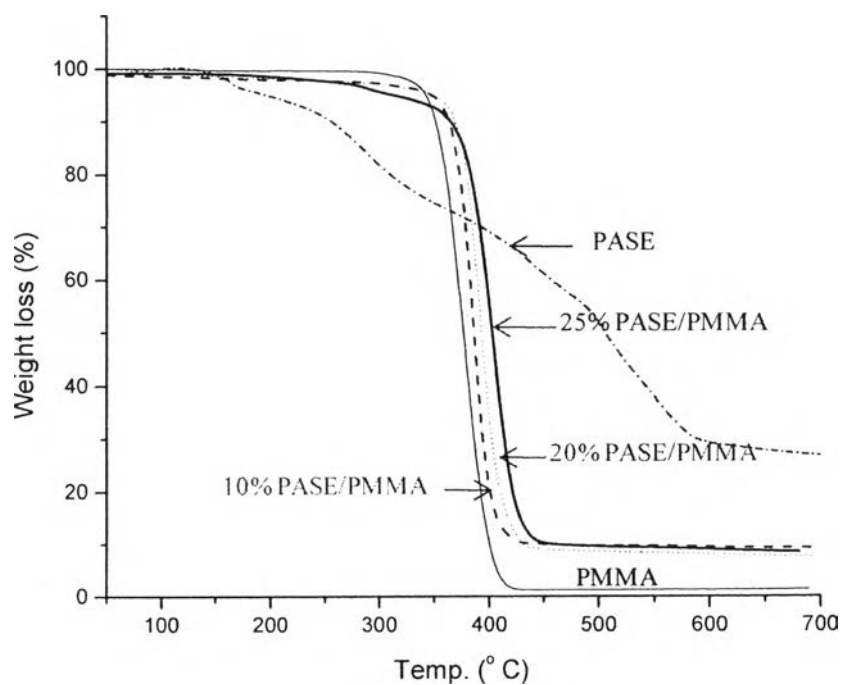


Figure 5.4TGA thermogram of claddings— PMMA and PASE/PMMA blends.

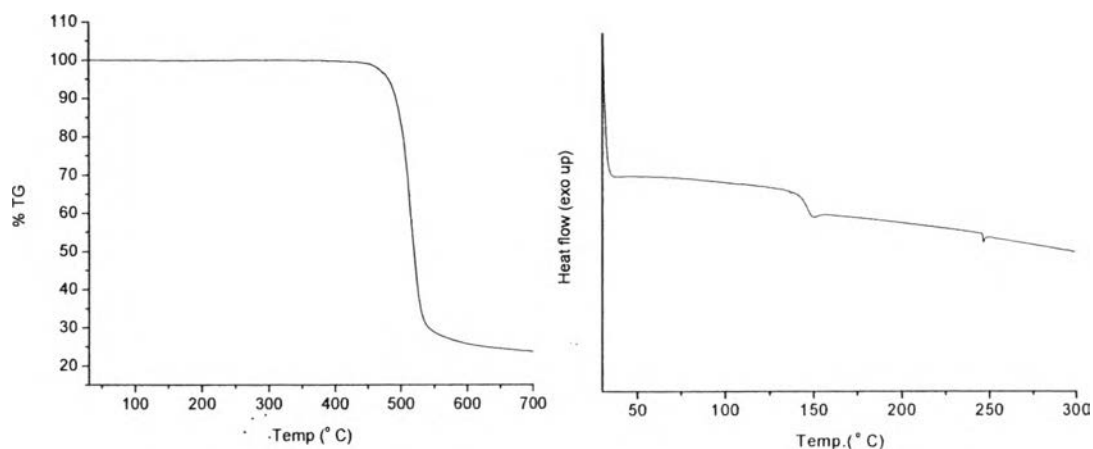


Figure 5.5 DSC and TGA thermograms of PC.

5.4.2 Co-extrusion of fiber

5.4.2.1 *Co-extrusion processing study*

The processing range extends from above the glass transition temperature to the thermal stability limit. The single screw extruder which was used to fabricate the core can operate at the shear stress less than 55 N/m^2 . Screw speed is one parameter that affect on the shear stress. Because PC is highly rigid polymer, it can create high shear stress when increasing screw speed. High temperature was needed to process one. Increasing the temperature at the feed zone, mixing zone and metering zone are a selected way to overcome the high shear stress problem. Table 5.2 show the shear stress, pressure drop at each processing temperature of PC processing. The lowest processing temperature and the highest screw speed of extruder that can process PC at shear stress lower than the maximum is 270, 285, 280 and 225°C (for feed zone, melting zone, metering zone and die, respectively) at 3 rpm of screw speed.

The optimum point for processing of single screw can determine from the graph of screw characteristic and die characteristic which is the relationship between pressure drop and flow rate. The flow rate and pressure drop in the metering zone and in the die are found by determining the value of the pressure drop for which the flow rates in the metering zone and the die are equal. The pressure drop and shear stress were obtained from the controller. The volumetric flow rate (Q) was calculated from the mass output from the following equation.

$$Q = \frac{\text{mass output}}{\text{density}}$$

From the result as shown in table 5.2, the process cannot operate at higher than 3 rpm of screw speed even increase the die temperature to 290 ° C so the pressure drop also cannot vary. The characteristic graph cannot create but the limiting of screw speed and temperature for fabricate PC were obtained. However, the optimum processing parameters also depend on properties of used-material explained in the further.

5.4.2.2 Processing temperature study

Since the temperature of core and cladding die is the same, the flowing of cladding at that temperature are also considered. The formation of fibers is a careful balance between the miscibility of the polymer melts and polymer viscosity (Mignanelli M., *et al.*, (2007)). The viscosity is a function of temperature and shear rate. PC at 280 ° C and PMMA at 260 ° C, only at 1000 s⁻¹ of shear rate PC and PMMA have the same viscosity at about 200 Pa.s. (Vannessa G., (2004)). In the fact that at 260 ° C of die, PMMA has too low viscous until it cannot form circular tube to cover around the PC core. Therefore this work, the die cannot have the temperature higher than these. The viscosity of PC, PMMA and PASE/PMMA were determine by using capillary rheometer at 225 – 250 °C at 10-10,000 s⁻¹ shear rate. The shear rate and viscosity relations of PC and PMMA were shown in the figure 5.5. It is difficult to obtain the same viscosity of PC and PMMA at the same temperature and shear rate. At 225 °C, the different ratio of viscosities is the lowest. So the die temperature used for fabrication is 225 °C. The processing temperatures of single screw form feed zone to die zone are 270, 285, 280 and 225 ° C at constant screw speed (3 rpm). The barrel temperature is 235 ° C which is higher than the die zone in order to reduce pressure from forcing of piston. Figure 5.6 shows that the viscosity of PASE/PMMA blends at 225 ° C are closely to PMMA. Therefore the temperature used to process PASE/PMMA is the same.

Table 5.2 shows the shear stress, pressure drop of PC processing.

Temperature (° C) from feed zone to die zone	screw speed (rpm)	pressure drop (psi)	shear stress (N/m ²)	Throughput rate (g/sec)	flow rate (mm ³ /sec)
275, 285, 285, 250	3	3.8	30	0.07723	64.36111
	5	*	*	*	*
275, 285, 280, 240	3	4	44	0.07243	60.36527
	5	4.9	*	*	*
275, 285, 280, 235	3	5	52	0.06977	58.14861
	5	**	**	**	**
275, 285, 275, 230	3	**	**	**	**
275, 285, 270, 225	3	**	**	**	**
275, 285, 275, 225	3	**	**	**	**
275, 285, 280, 225	3	5.5	34	0.06950	57.92361
	5	**	**	**	**

Note : * single screw can operate less than 60 second

** single screw cannot operate

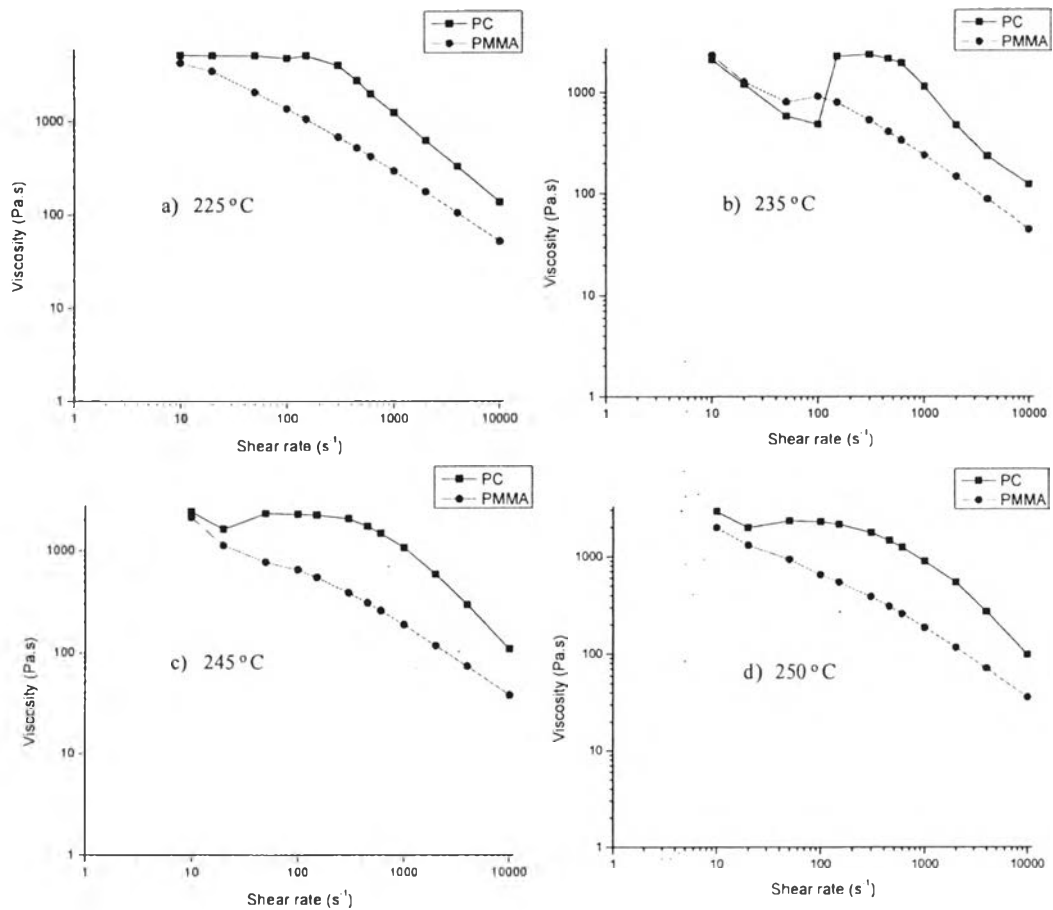


Figure 5.6 Viscosities of PC and PMMA at different temperatures by capillary rheometer (Raw data is shown in appendix C).

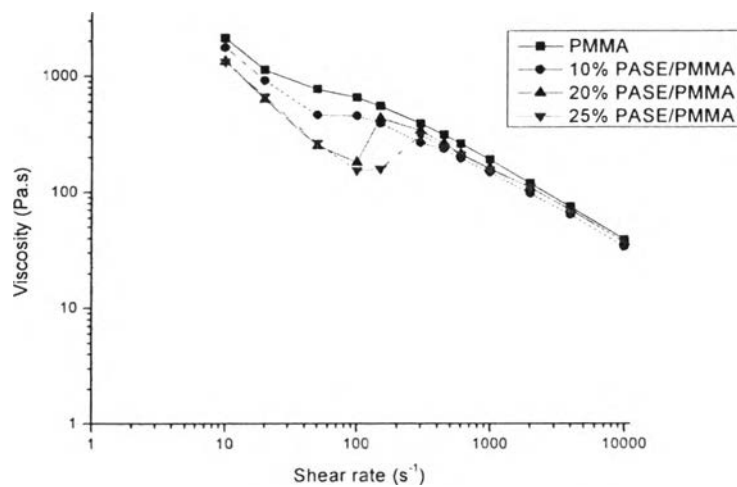


Figure 5.7 Viscosities of PMMA and PASE/PMMA at 225 °C.

5.4.3 Fiber's morphology

5.4.3.1 Core Diameter and Cladding Thickness

The diameter requirement of core is in the same range of commercial optical fiber. ESKA is PMMA-core optical fiber produced by Misubishi Rayon has 1.00 mm fiber diameter—0.98 mm core diameter and 0.02 mm cladding thickness. The diameters of PC core were studied by varying draw ratio at free falling, 20 rpm, 30 rpm, 40 rpm, 50 rpm and 55 rpm. Figure 5.7 shows the graph of diameter and draw ratio. At 30, 40, 50 and 55 rpm, the diameters of fiber are too small. So the draw ratio at 20 rpm (839.91 μm .) and free falling (1205.89 μm .) (see in table 5.3) were selected to use in the process.

Table 5.3 Diameter of PC fiber at various draw ratio

Draw ratio (rpm)	Diameter of PC fiber (μm .)
0 (free falling)	1205.89 \pm 4.05
20	839.91 \pm 3.14
30	573.53 \pm 2.38
40	568.43 \pm 2.72
50	556.13 \pm 2.13
55	521.48 \pm 2.55

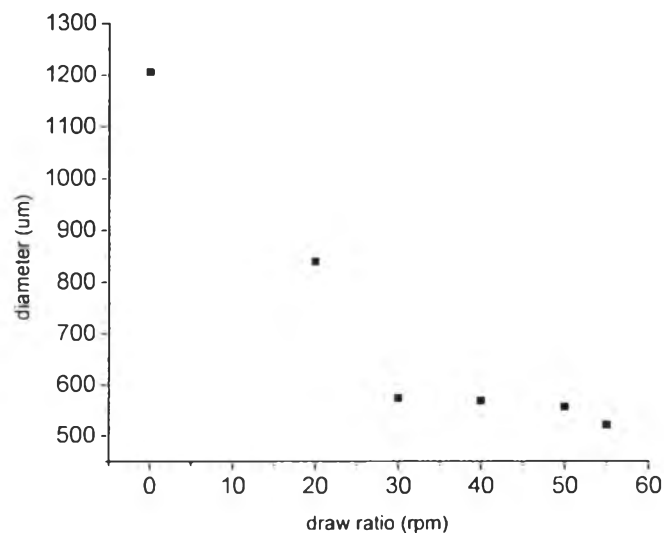


Figure 5.8 Graph of diameter of PC fiber at various draw ratios.

Diameters of fibers at free falling are in the range of 1.1-1.4 mm. Core diameters are about 0.99-1.3 mm which is bigger than die diameter (1mm.) due to swelling effect. Cladding thicknesses are about 65-97 μm . which are depend on the piston speed. Cladding thickness tend to increase when the piston speed increase. The thickness of claddings is also less than the width circular sheath die (0.7 mm.) because of forcing from core driving. Diameters of fibers at 20 rpm draw ratio are in the range of 0.83-0.98 mm. Core diameters are about 0.73-0.89 mm which is smaller than diameter of fibers at free falling condition (1mm) because of higher drawing. Cladding thickness at 20 mm/min piston speed is about 40-72 μm and at 24.5 mm/min piston speed are about 63-95 μm .

The pictures of PMMA-cladding type fiber from optical microscope at 4x of magnification (Fig.5.8) and also in SEM image SEM (Fig.5.9) cannot see the boundary of core and cladding. At 20x of magnification can see one but it not clearly. 0.3 % CaCO_3 by weight was mixed into the PMMA in the barbender at 190 ° C to be a cladding material in order to prove that PMMA and PC melt do not mixed together. CaCO_3 /PMMA cladding was process at 245 ° C of barrel temperature and 250 ° C of die temperature because CaCO_3 act as filler and made PMMA blend become higher viscosity. The SEM images and optical microscope pictures can prove that hypothesis(Fig. 5.10). The images show clearer boundary between core and cladding. The reason of unclary boundary is that PC and PMMA are compatible polymers because of good interaction of phenyl ring of PC and carbonyl groups of PMMA (Moussaif N., *et al.*, 1999) so they have merged together at the interface. This reason was confirm by Liu's research. PC and PMMA were fabricated to form sandwich by co-extrusion process. They found that the contact of two polymers is not imperfectly sharp interface. The force assembly by co extrusion made it possible to create the mixing at the interface region and to decrease the outer layer (Liu R.Y.F., *et al.*, (2005)). The mixing between core and cladding at the boundary made tough PC core become brittle as reported in mechanical properties. Furthermore, this would be the defect when light transmitted though the fiber which called microbending loss (Farrell, 2002). But the refractive index does not change very much from those of the pure component because of good miscibility (Rajuru A.V., *et al.*, (2000)). Figure 5.11, 5.12 and 5.13 show the optical microscope images

of 10% PASE/PMMA-cladding type, 20% PASE/PMMA-cladding type and 25% PASE/PMMA-cladding type fiber, respectively. The obtained fibers have very thin cladding at about 40-90 μm comparing to the commercial fiber such as ESKA which has 0.2 mm cladding thickness. The pictures show that the boundary between core and cladding is not sharp and the surface of fiber is not smooth. The core surface of 20% PASE/PMMA-cladding type fiber at 20 rpm of draw ratio and 24.5 mm/min of piston speed is not smooth which may be affected by the optical properties. However, this cladding type at free falling and 24.5 mm/min of piston speed the fiber has concentric shape. The dimensions of the fibers are different. The reason is the viscosity difference so the flow behavior is different. The viscosity ratio between the core and cladding material has an impact on the interface of them. The interfacial effects are observed with increase in piston speed because polymers have both viscous and elastic properties (Vannessa G., (2004)).

Table 5.4 Diameter of fiber, core and thickness of cladding

Cladding type	Piston speed (mm./min)					
	20			24.5		
	core d.a. ($\mu\text{m.}$)	cladding thickness ($\mu\text{m.}$)	fiber d.a. ($\mu\text{m.}$)	core d.a. ($\mu\text{m.}$)	cladding thickness ($\mu\text{m.}$)	fiber d.a. ($\mu\text{m.}$)
Free falling						
PMMA	1224.39 ± 17.35	79.08 ± 7.63	1355.03 ± 14.53	1359.48 ± 22.48	95.39 ± 5.343	1422.66 ± 28.38
10% PASE/PMMA	965.57 ± 17.80	66.21 ± 4.17	1103.79 ± 10.05	1190.54 ± 13.45	76.72 ± 5.81	1278.87 ± 8.94
20% PASE/PMMA	997.48 ± 14.55	74.43 ± 1.79	1110.63 ± 13.42	1267.72 ± 14.89	86.75 ± 5.26	1313.87 ± 11.71
25% PASE/PMMA	1057.65 ± 10.58	97.21 ± 6.48	1139.19 ± 13.39	—		
20 rpm draw ratio						
PMMA	844.37 ± 14.56	56.56 ± 4.97	879.96 ± 28.65	855.01 ± 12.31	63.2 ± 9.82	956.58 ± 16.56
10% PASE/PMMA	734.26 ± 19.54	72.94 ± 4.22	838.44 ± 28.59	897.62 ± 10.52	85.14 ± 4.08	971.03 ± 11.47
20% PASE/PMMA	881.93 ± 14.50	40.39 ± 3.11	914.29 ± 10.62	889.07 ± 9.54	65.39 ± 8.73	984.45 ± 16.36
25% PASE/PMMA	—			884.58 ± 11.37	67.16 ± 3.95	954.17 ± 12.62

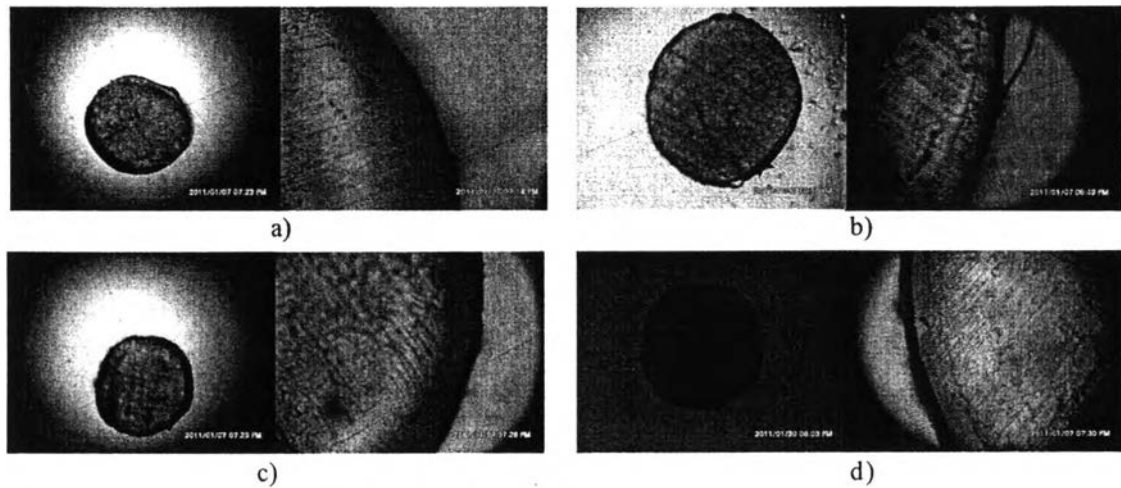


Figure 5.9 Cross-section from optical microscope of PMMA-cladding type fibers in different draw ratio and piston speed ratio (4x: left picture and 20x: right picture); a) free falling and 20 mm/min of piston speed, b) free falling and 24.5 mm/min of piston speed, c) 20 rpm of draw ratio and 20 mm/min of piston speed and d) 20 rpm of draw ratio and 24.5 mm/min of piston speed.

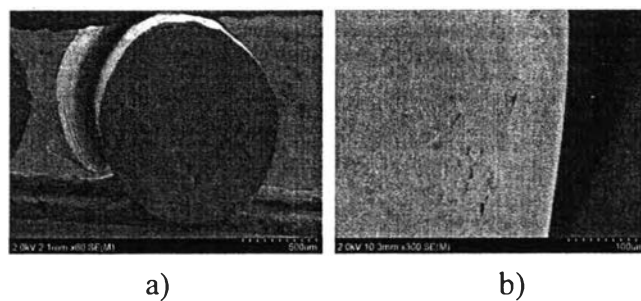


Figure 5.10 SEM images of cross-section of PMMA-cladding type fiber; a) 500 μm , b) 100 μm).

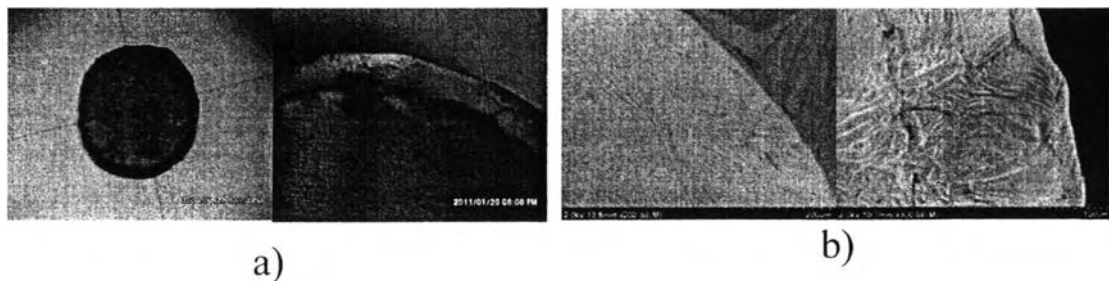


Figure 5.11 a) Optical microscope and b) SEM images of cross-section of $\text{CaCO}_3/\text{PMMA}$ -cladding type fiber (200 and 100 μm).

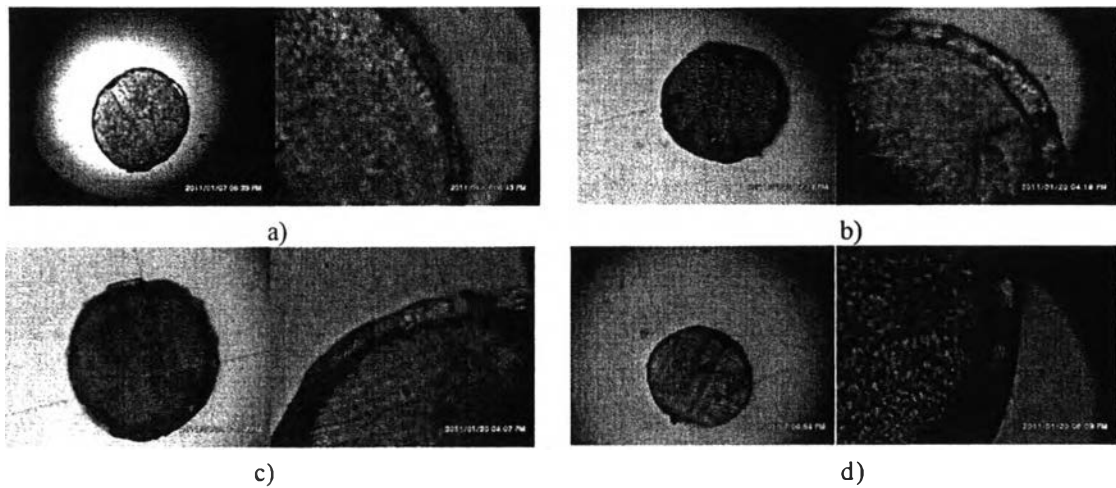


Figure 5.12 Cross-section from optical microscope of 10% PASE/PMMA-cladding type fibers in different draw ratio and piston speed ratio (4x: left picture and 20x: right picture); a) free falling and 20 mm/min of piston speed, b) free falling and 24.5 mm/min of piston speed, c) 20 rpm of draw ratio and 20 mm/min of piston speed and d) 20 rpm of draw ratio and 24.5 mm/min of piston speed.

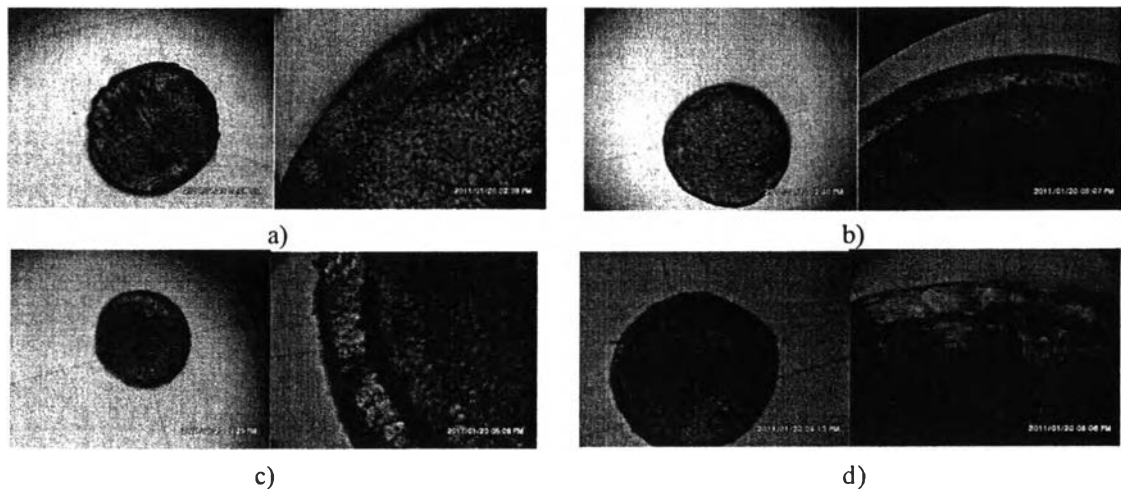


Figure 5.13 Cross-section from optical microscope of 20% PASE/PMMA-cladding type fibers in different draw ratio and piston speed ratio (4x: left picture and 20x: right picture); a) free falling and 20 mm/min of piston speed, b) free falling and 24.5 mm/min of piston speed, c) 20 rpm of draw ratio and 20 mm/min of piston speed and d) 20 rpm of draw ratio and 24.5 mm/min of piston speed.

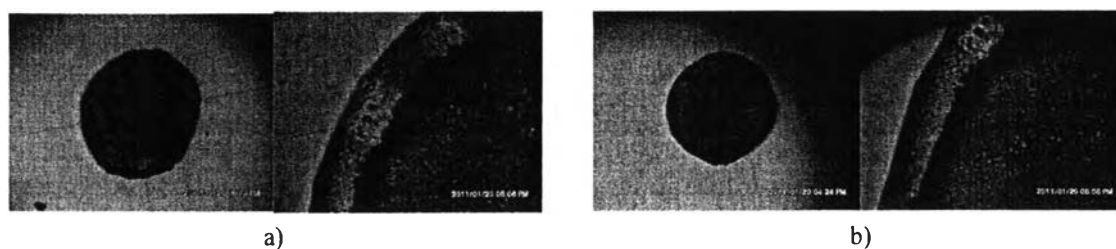


Figure 5.14 Cross-section from optical microscope of 25% PASE/PMMA-cladding type fibers in different draw ratio and piston speed ratio (4x: left picture and 20x: right picture); a) free falling and 24.5 mm/min of piston speed and b) 20 rpm of draw ratio and 24.5 mm/min of piston speed.

The images from SEM show that some fibers have bubbles between the interface of core and cladding because the die's design have a circular metal at boundary of core and cladding, so the melt core and cladding counteract outside the die so air can penetrate into the interface of them.

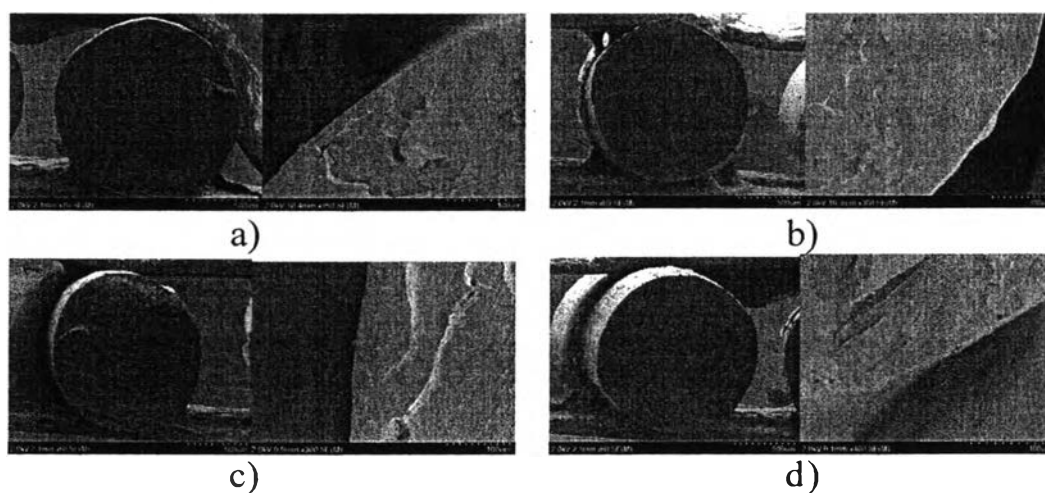


Figure 5.15 SEM images of cross-section of 10% PASE/PMMA-cladding type fiber (500 μm and 100 μm); a) free falling and 20 mm/min of piston speed, b) free falling and 24.5 mm/min of piston speed, c) 20 rpm of draw ratio and 20 mm/min of piston speed and d) 20 rpm of draw ratio and 24.5 mm/min of piston speed.

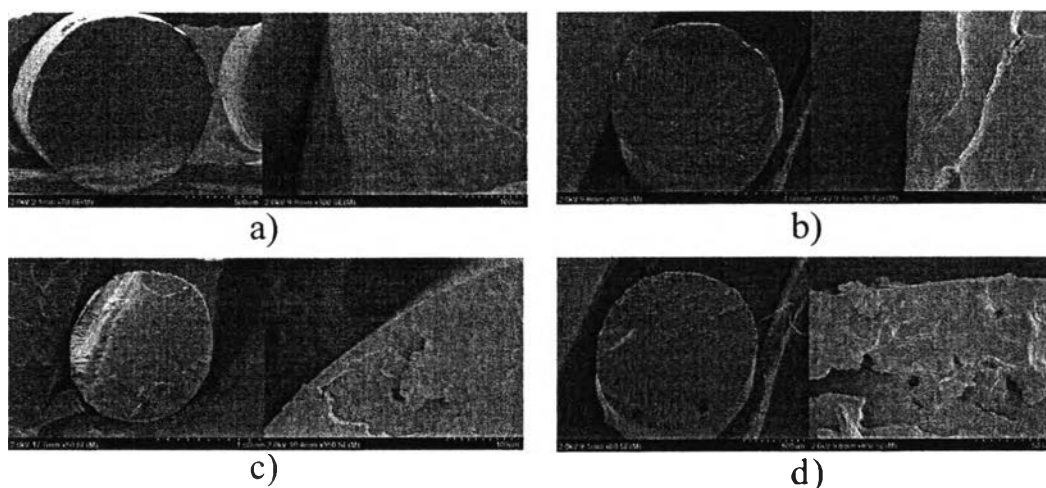


Figure 5.16 SEM images of cross-section of 20% PASE/PMMA-cladding type fiber; a) free falling and 20 mm/min of piston speed (500 μm and 100 μm), b) free falling and 24.5 mm/min of piston speed (1.00 mm and 100 μm), c) 20 rpm of draw ratio and 20 mm/min of piston speed (1.00 mm and 100 μm) and d) 20 rpm of draw ratio and 24.5 mm/min of piston speed (500 μm and 50 μm).

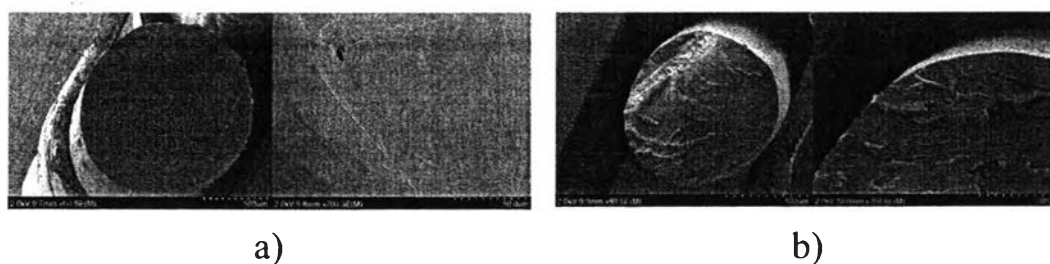


Figure 5.17 SEM images of cross-section of 25% PASE/PMMA-cladding type fiber; a) free falling and 20 mm/min of piston speed (500 μm and 50 μm) and b) 20 rpm of draw ratio and 24.5 mm/min of piston speed (500 μm and 200 μm).

5.4.4 Mechanical properties of fibers

The stress-strain curves of the fibers show in the Figure 5.17. The graph of 20% and 25% PASE/PMMA-cladding type fibers have two yield points resulting from drawing of brittle material—out side cladding and ductile material—PC core. All of PMMA-cladding type fibers and 10% PASE/PMMA-cladding type of free falling, 20 mm/min of piston speed and 20 rpm of draw ratio, 24.5 mm/min piston speed do not show plastic deformation which is the characteristic of brittle

material (Ward, I.M., 1983). However, 10% PASE/PMMA-cladding type of free falling, 24.5 mm/min of piston speed and 20 rpm of draw ratio, 20 mm/min of piston speed have two yield point and high elongation because fiber at free falling, 24.5 mm/min of piston speed has the big core diameter and fiber at 20 rpm of draw ratio, 20 mm/min of piston speed has the lowest cladding thickness, therefore PC's properties are dominate. PASE/PMMA-cladding type fibers show percentage of strain higher than PMMA-cladding type. This implies that PASE/PMMA-cladding fibers are tougher than PMMA-cladding type fiber. However, comparing to PC fiber, they still brittle as show in figure 5.18. Although they have the tough PC inside, the brittle cladding can induce PC core crack (Ebert, *et al.*, 2004).

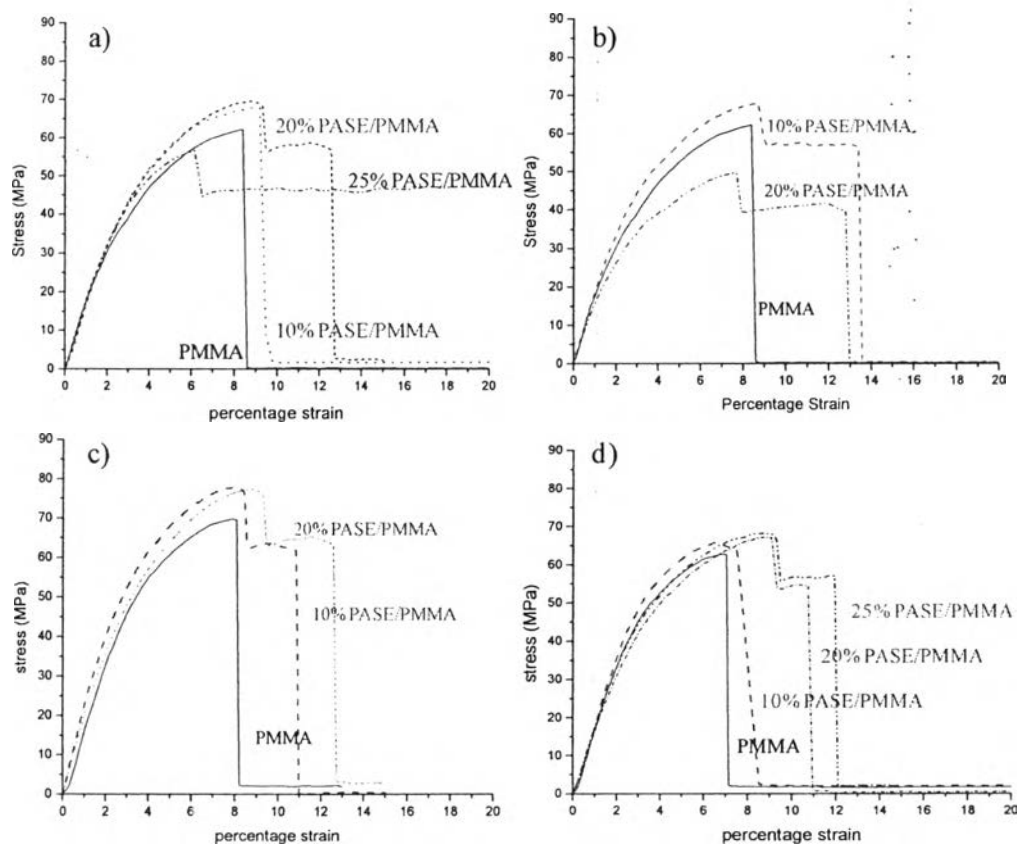


Figure 5.18 Stress-strain curve of obtained fiber at various draw ratio and piston speed; a) free falling and 20 mm/min of piston speed, b) free falling and 24.5 mm/min of piston speed, c) 20 rpm of draw ratio and 20 mm/min of piston speed and d) 20 rpm of draw ratio and 24.5 mm/min of piston speed.

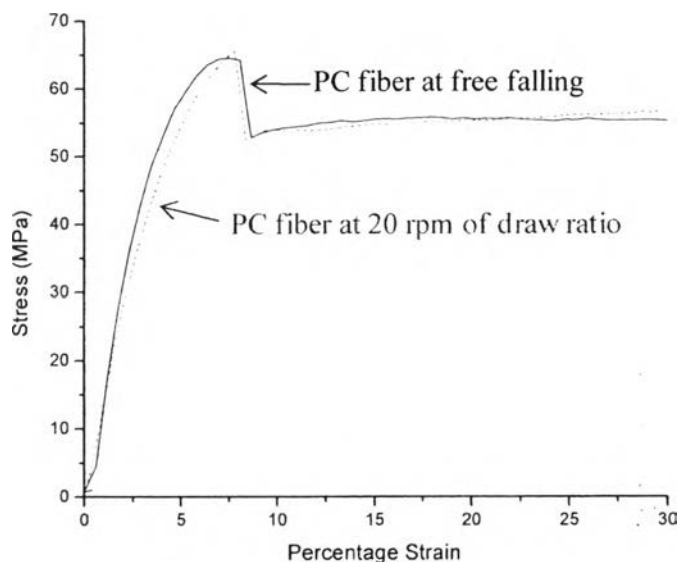


Figure 5. 19 Stress-strain curve of PC fiber at free falling and 20 rpm of draw ratio.

The Young's modulus and stress at yield of the fibers which refer to the elastic region and stiffness of polymer are not exactly trend. However, the stress and Young's modulus of them are indifferent. Table 5.4 show the Young's modulus, stress at yield and percent strain at yield of fiber at various processing parameters. Young's modulus and tensile strength of all type fibers are in the same range of pure PC (Young's modulus of PC— 2-2.4 GPa, Tensile strength of PC— 55-75 MPa). The obtained fibers also have tensile strength close to other research such as Guerrero H., *et al* (1998)—tensile strength = 58.7 ± 0.9 MPa and Orth P., *et al.* (1998)—tensile strength = 55 MPa. The tensile strength of the fibers also close to the ESKA CK40— tensile strength = 65 MPa.

Table 5.5 Summary of fiber mechanical properties

Cladding type	Piston speed (mm./min)									
	20					24.5				
	core d.a. ($\mu\text{m.}$)	cladding thickness($\mu\text{m.}$)	Modulus (MPa)	Stress at yield (MPa)	% Strain at yield	core d.a. ($\mu\text{m.}$)	cladding thickness ($\mu\text{m.}$)	Modulus (MPa)	Stress at yield (MPa)	% Strain at yield
Free falling										
PMMA	1224.39 ± 17.35	79.08 ± 7.63	1814.2 ± 126.62	60.8 ± 1.12	9.62 ± 0.37	1359.48 ± 22.48	95.39 ± 5.343	1984.2 ± 141.51	68.01 ± 3.81	8.99 ± 3.30
10% PASE/PMMA	965.57 ± 17.80	66.21 ± 4.17	2195.97 ± 269.22	59.27 ± 6.59	8.38 ± 0.41	1190.54 ± 13.45	76.72 ± 5.81	1977.38 ± 80.25	63.73 ± 3.81	7.95 ± 0.60
20% PASE/PMMA	997.48 ± 14.55	74.43 ± 1.79	1518.87 ± 134.96	55.62 ± 6.59	8.5 ± 0.41	1267.72 ± 14.89	86.75 ± 5.26	2049.37 ± 119.08	50.41 ± 6.27	7.04 ± 0.84
25% PASE/PMMA	1057.65 ± 10.58	97.21 ± 6.48	2045.14 ± 87.46	60.57 ± 3.97	5.77 ± 0.69	—				
PC	1205.89 ± 4.05		1980.2 ± 59.63	65.59 ± 2.57	8.12 ± 0.58	—				
20 rpm draw ratio										
PMMA	844.37 ± 14.56	56.56 ± 4.97	1837.4 ± 172.82	63.76 ± 4.18	8.74 ± 0.61	855.01 ± 12.31	63.2 ± 9.82	2112.48 ± 124.93	70.32 ± 3.72	7.63 ± 0.43
10% PASE/PMMA	734.26 ± 19.54	72.94 ± 4.22	2382.22 ± 110.06	74.75 ± 5.22	7.84 ± 0.61	897.62 ± 10.52	85.14 ± 4.08	1740.85 ± 34.6	51.74 ± 3.91	8.44 ± 0.57
20% PASE/PMMA	881.93 ± 14.50	40.39 ± 3.11	2218.33 ± 88.75	65.84 ± 2.26	8.64 ± 0.26	889.07 ± 9.54	65.39 ± 8.73	2495.45 ± 109.73	64.66 ± 3.65	7.82 ± 0.14
25% PASE/PMMA			—			884.58 ± 11.37	67.16 ± 3.95	1855.36 ± 128.55	59.5 ± 1.09	8.56 ± 0.15
PC	839.91 ± 3.14		1954.7 ± 76.91	64.6 ± 2.45	8.26 ± 0.34	—				

5.5 Conclusion

The claddings of this optical fiber are obtained by mixing PASE with PMMA. The blending is a good compatibility and behaves more flexible than pure PMMA. The fibers were produced by co-extrusion process. Some of the obtained fibers have not good shape; some fibers have bubble inside them. The dimensions of fibers are not so quite difference even the processing parameter were varied. The cladding can induce PC core fibers to brittle fiber. Young's modulus and tensile strength of all type fibers are in the same range of pure PC. The obtained fibers also have tensile strength close to the research of such as Guerrero H., *et al* (1998) and Orth P., *et al.* (1998).

5.6 Acknowledgements

First of all, I would like to thank PTT Phenol Company Limited for supporting the thesis work. Also thank the Polymer Processing and Polymer Nanomaterials Research Unit; Chulalongkorn University.

In addition, I gratefully acknowledge the help of Assoc. Prof. Rathanawan Magaraphan, Dr. Satida Krailas and Dr. Sarawut Lunvongsa for the suggestion of the experiment.

Finally, the author is grateful for the scholarship and funding of the thesis work provided by the Petroleum and Petrochemical College; and Center for Petroleum, Petrochemicals, and Advanced Materials.

5.7 References

1. Guerrero, H., Guinea, G.V., Zoido, J. (1998) Mechanical properties of polycarbonate optical fibers. Fiber and Integrated Optics, 17, 231-2424

2. Liu R.Y.F., Ranade A.P., Wang H.P., Hiltner A., and Baer E. (2005) Force Assembly of Polymer Nanolayers Thinner than the interphase. Macromolecules, 38, 10721-10727
3. Mignanelli M., Wani K., Ballato J., Foulger S., and Brown P. (2007) Polymer microstructure fibers by one-step extrusion. Optic express, 15, 6183
4. Rajuru A.V. and Reddy R.L. (2000) Miscibility studies of Polycarbonate/Poly(methyl methacrylate) and Polycarbonate/Polystyrene Blends as Measured by Viscosity, Ultrasonic, and Refractive Index Methods. J. Polym. Anal. Charact., 5, 467-473
5. Sung I.S. and Park C.W. (2001) Diffusion-assisted coextrusion process for the fabrication of graded-index plastic optical fibers. Ind. Eng. Chem. Res., 40, 3740-3748
6. Vanessa G. (2004) Practical Guide to injection molding. ISBN 978-1-85957-444-7, 227
7. Ward I.M. and Sweeney J. (1983) Mechanical Properties of Solid Polymers, second edition, New York: John Wiley, 56-97